

## Domain Observation of $\text{Pb}(\text{Mg}_{1/3}\text{Nb}_{2/3})\text{O}_3\text{-PbTiO}_3$ Single Crystals in a Vacuum by Contact Resonance Piezoresponse Force Microscopy

Hirotake Okino, Takuya Matsushita and Takashi Yamamoto

Department of Communications Engineering, National Defense Academy, Kanagawa 239-8686, Japan

Fax: +81-468-44-5911, E-mail: hokino@nda.ac.jp

The domain structure images of a (001) plate of  $\text{Pb}(\text{Mg}_{1/3}\text{Nb}_{2/3})\text{O}_3\text{-PbTiO}_3$  (PMN-PT) single crystal were successfully obtained in a vacuum using contact resonance piezoresponse force microscope (CR-PFM). Although the Curie temperature of the sample was approximately 135 °C, the same fingerprint-shaped domain images were observed up to 175 °C. We also found spot-shaped domains tens of nanometers in diameter at temperatures above 175 °C. Once these spot-shaped domains appeared, they were observed even below the Curie temperature and returned gradually to the large fingerprint-shaped domains obtained before the sample heating. This long time relaxation phenomenon implied a relationship to the relaxor characteristics.

Key words: piezoresponse force microscopy; domain imaging; contact resonance; relaxor ferroelectrics; PMN-PT;

### 1 INTRODUCTION

After Smolensky *et al.*<sup>1,2)</sup> have found  $\text{Pb}(\text{Mg}_{1/3}\text{Nb}_{2/3})\text{O}_3$  (PMN), there has been remarkable interest in relaxor ferroelectric materials owing to their peculiar characteristics, so called 'relaxor characteristics': huge permittivity, giant piezoelectric constant, broad dispersion of permittivity and dull variation of spontaneous polarization. Particularly, after Kuwata *et al.*<sup>3)</sup> has reported an electromechanical coupling factor  $k_{33}$  of 92% and a piezoelectric constant  $d_{33}$  of 1500 pC/N for  $0.91\text{Pb}(\text{Zn}_{1/3}\text{Nb}_{2/3})\text{O}_3\text{-}0.09\text{PbTiO}_3$  (PZN-9%PT), relaxor ferroelectric single crystals have been attracting considerable attention for medical imaging and actuator applications.<sup>4,5)</sup> From the early 1990s, the motivation to employ relaxors for such applications has driven not only the improvement of single crystal growth techniques but also experimental and theoretical investigations on the relaxor characteristics.

Although an unified model which can explain the whole relaxor characteristics consistently has not been provided yet, the relaxor characteristics have been discussed and have mostly been understood in terms of microdomains (polarized micro clusters). The microdomains were the evidence of the lack of long-range order and originated from non-uniform crystalline field due to local fluctuation of distribution of B site cation composition.<sup>6)</sup> The microdomains have been studied well using crystal structure analysis techniques such as neutron diffraction method,<sup>7,8)</sup> extended X-ray absorption fine structure method<sup>9)</sup> and X-ray diffuse scattering method.<sup>10)</sup> Using these techniques, huge permittivity of relaxor ferroelectrics was examined from the viewpoint of ion displacement in crystal. Besides, transmission electron microscope (TEM)

have been a representative technique for real space observations of the microdomains owing to its high resolution and capability for investigating dynamic phenomena.<sup>11)</sup> However, TEM could not visualize 180° domain boundaries.

We have investigated domain structures of relaxor ferroelectric single crystals using piezoresponse force microscope (PFM)<sup>12,13)</sup> to understand the relationship between real space domain structures and the relaxor characteristics.<sup>14,15)</sup> In spite of lower resolution than TEM, PFM had an ability to visualize 180° domain boundaries, and was easier to operate than TEM.

In our previous work,<sup>15)</sup> we have observed domain structure images of the (001) plate of a  $\text{Pb}(\text{Mg}_{1/3}\text{Nb}_{2/3})\text{O}_3\text{-PbTiO}_3$  (PMN-PT) single crystal in an air at various temperatures using contact resonance piezoresponse force microscope (CR-PFM). Domain imaging became more difficult with increasing sample temperature, because applied modulation voltage caused ferroelectric polarizations reversal more easily at higher temperatures. In order to address this issue, we adapted contact resonance mode<sup>16)</sup> which could amplify piezoresponse signals, and successfully obtained PFM images at higher sample temperatures (>200 °C). However, there was a moot point that even above the Curie temperature, we recorded the same domain images as obtained below the Curie temperature. We assumed that owing to air convection, the surface temperature of the sample still remained below the Curie temperature even after bulky phase transition to paraelectric phase underwent. In addition, the air convection degraded the S/N ratio of piezoresponse signals and made domain images noisy.

In this article, in order to clear the air convection problem, we observed the domain structures of the PMN-PT single crystal in a vacuum.

## 2 EXPERIMENTAL

During PFM observations, domains were visualized by detecting inverse piezoelectric oscillations caused by a modulation sinusoidal voltage applied between a conducting tip and an electrode on the backside of the sample.<sup>13)</sup> These vibrations resulted in the cantilever deflection owing to the tip in contact with the ferroelectric sample surface. This modulated cantilever deflection was acquired and amplified using a lock-in amplifier. Accordingly, it was possible to determine the projection of the polarization vector onto vertical direction.

The only difference between PFM and CR-PFM was the frequency of the modulation signal. In the contact resonance mode, the frequency of modulation signals were maintained at the resonance frequency of cantilever deflection when in contact with a sample surface. Utilizing contact resonance, we could improve the S/N ratio of piezoresponse signals and operate PFM imaging with lower amplitude of the modulation signal. The details of PFM and CR-PFM imaging principle have been described elsewhere.<sup>14,17)</sup>

The experimental setup of CR-PFM consisted of a commercial scanning probe microscope (JEOL, JSPM-4210) connected to a lock-in amplifier (NF Electronic Instruments, LI-575) and a oscillator (NF Electronic Instruments, WF1945). The sample stage of the JSPM-4210 was temperature-controlled by a ceramic heater, while the SPM was maintained in a vacuum ( $< 1.0 \times 10^{-3}$  Pa) using a turbo molecular pump. Si cantilevers used for domain visualization (Mikro Masch, NSC-12-E/CR-AU) were coated with Au/Cr, which had a length of  $350 \mu\text{m}$ , a thickness of  $2.0 \mu\text{m}$ , a spring constant of  $0.25 \text{ N/m}$  and a free resonance frequency of  $20 \text{ kHz}$ . The amplitude of the applied modulation signal was  $0.2 V_{pp}$ .

PMN-PT single crystals with practically morphotropic phase boundary composition (the composition rate of PT  $\approx 32\%$ ) were grown by the Bridgman method. Obtained PMN-PT ingot was sliced into  $0.5 \text{ mm}$  thick (001) plates. Pt/Ta electrodes were deposited on the backside of the samples by rf-sputtering. The Curie temperature of the specimens was approximately  $135^\circ\text{C}$  estimated from permittivity measurements.

## 3 RESULTS AND DISCUSSION

Figure 1 shows the frequency spectra of piezoresponse signals around the 1st mode contact resonance frequency measured at various temperatures: (a) R.T., (b)  $125^\circ\text{C}$ , (c)  $150^\circ\text{C}$  and (d)  $175^\circ\text{C}$ . During the measurement, the tip of the cantilever NSC-12-E/CR-AU was in contact with the (001) plate PMN-PT. The measured frequency spectra were stable up to  $175^\circ\text{C}$  because of the absence of the air convection. Changes in the resonance frequencies within  $\pm 0.5 \text{ kHz}$  were due to fluctuations of imaging force.

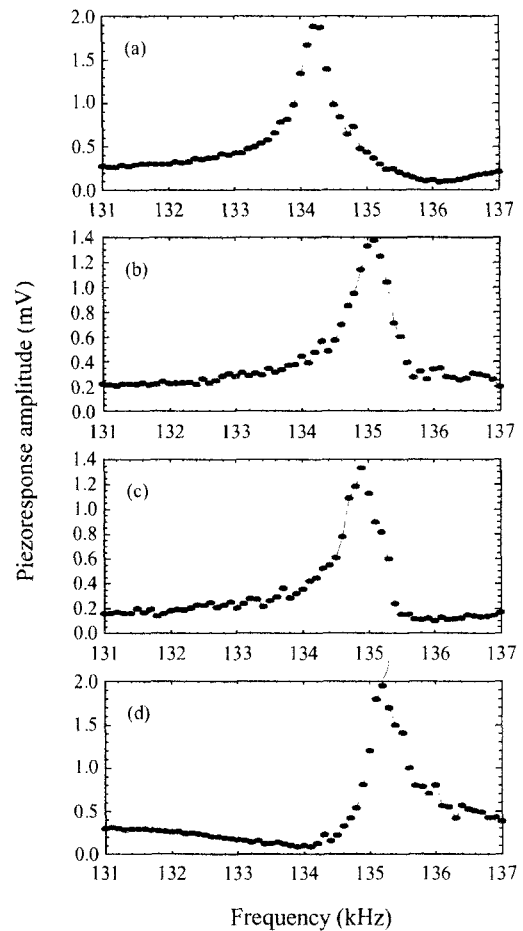


Fig. 1 The frequency spectra of piezoresponse signals around the 1st mode contact resonance frequency measured at various temperatures: (a) R.T., (b)  $125^\circ\text{C}$ , (c)  $150^\circ\text{C}$  and (d)  $175^\circ\text{C}$ .

The domain images of the (001) plate PMN-PT single crystal were successfully acquired in a vacuum at temperatures up to  $205^\circ\text{C}$ . Figure 2(a) shows  $1.9 \mu\text{m} \times 1.9 \mu\text{m}$  topographic image of the sample. The surface of the PMN-PT plate was polished and the root mean square of surface roughness was  $3.1 \text{ nm}$ . Figure 2(b) through 2(e) are CR-PFM images obtained at various sample temperatures ranging from  $125^\circ\text{C}$  to  $205^\circ\text{C}$ . All these images were recorded at the same area with figure 2 (a). Here, white and black areas in CR-PFM images represent vertical polarization vectors which exit from and enter into the sample surface, respectively.

The same domain images were observed below and above the Curie temperature (figure 2 (b) and 2 (c)), which was similar to the result<sup>15)</sup> obtained in the atmosphere. This result denied our previous hypothesis that the sample surface temperature dropped below the Curie temperature because of the air convection. Another assumption was that the Curie temperature had local variation due to the non-uniformity of the PT composition rate. However, this issue was under discussion.

At temperatures above  $175^\circ\text{C}$  (figure 2 (d) and (e)), spot-shaped domains tens of nanometers in diameter

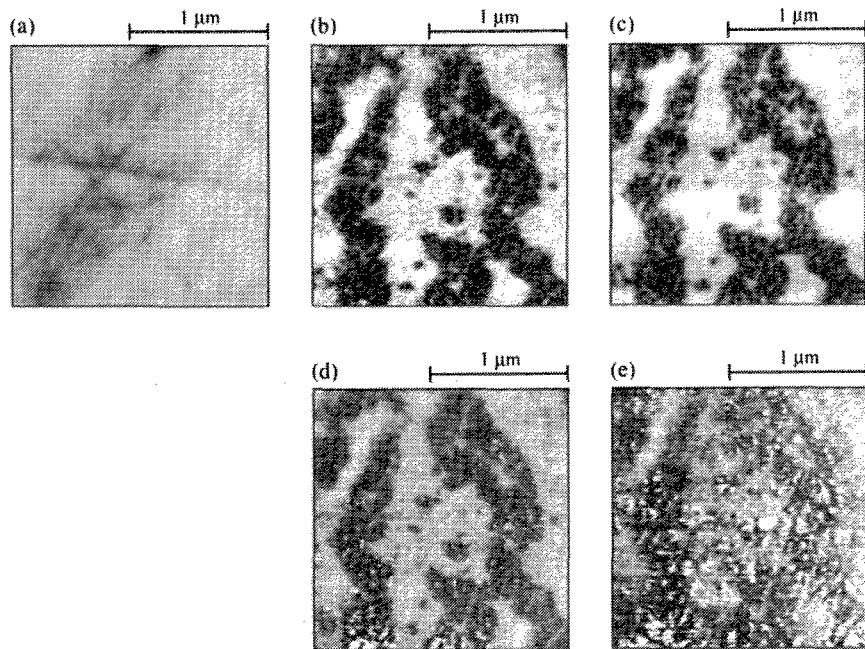


Fig. 2 (a) A  $1.9\mu\text{m}\times 1.9\mu\text{m}$  topographic image and (b)–(e) CR-PFM images of the (001) plate PMN-PT single crystal. The CR-PFM images were observed at (b): $125^\circ\text{C}$ , (c): $150^\circ\text{C}$ , (d): $175^\circ\text{C}$  and (e): $205^\circ\text{C}$ .

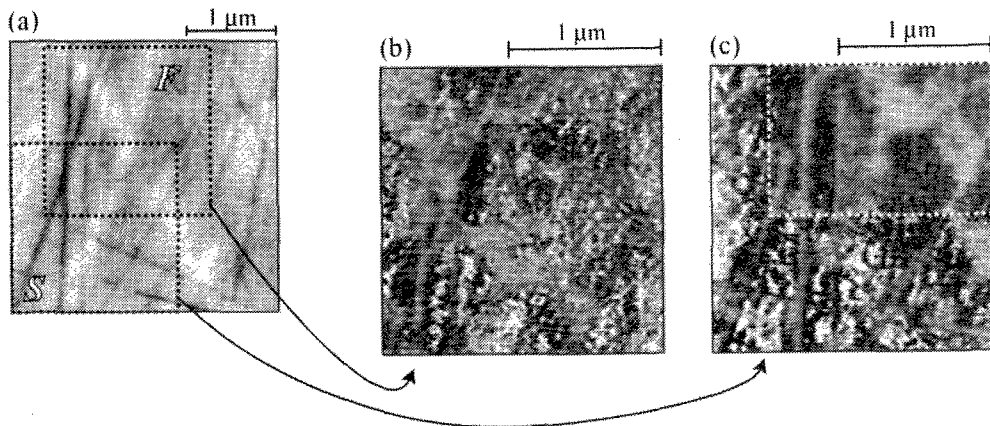


Fig. 3 (a) A  $3.0\mu\text{m}\times 3.0\mu\text{m}$  topographic image of the (001) plate PMN-PT single crystal. Area *F* and *S* is scanning area of Fig. 3 (b) and Fig. 3 (c). (b) A CR-PFM image obtained at  $105^\circ\text{C}$  in the area *F*. Before the observation, the sample was heated up to  $220^\circ\text{C}$  and then cooled down to  $105^\circ\text{C}$  at a rate of  $60^\circ\text{C}/\text{h}$ . (c) A CR-PFM image obtained in the area *S* successively after the first scan (Fig. 3 (b)).

emerged. Unfortunately, it was frequently difficult to record these domain patterns reproducibly in the same area (Figure 3). Figure 3(a) is a  $3.0\mu\text{m}\times 3.0\mu\text{m}$  topographic image of the specimen. Area *F* and *S* is scanning area of figure 3 (b) and 3 (c). Figure 3 (b) is a CR-PFM image obtained at  $105^\circ\text{C}$  in the area *F*. Before the observation, the sample was heated up to  $220^\circ\text{C}$  and then cooled down to  $105^\circ\text{C}$  at a rate of  $60^\circ\text{C}/\text{h}$ . Figure 3 (c) is a CR-PFM image obtained in the area *S* successively after the first scan (figure 3 (b)). In figure 3 (c), spot patterns were not observed in an overlapping area between the area *F* and *S*, indicating that applied modulation voltage erased spot-shaped patterns during the first scan. In order to ob-

serve these patterns reproducibly, the applied modulation voltage should be reduced again.

Once these spot-shaped domains appeared, they were observed even below the Curie temperature. Figure 4 shows  $1.9\mu\text{m}\times 1.9\mu\text{m}$  CR-PFM images observed after the sample was heated up to  $220^\circ\text{C}$  and then cooled down to  $50^\circ\text{C}$  at a rate of  $60^\circ\text{C}/\text{h}$ : Figure 4(a) through (c) were obtained just after the sample was cooled down, after 9 hours passed and after 18 hours passed, respectively. Because of the reproducibility problem described above, scanning areas of these images were different each other. After the cooling process, the spot-shaped domains returned gradually to the large fingerprint-shaped domains obtained before

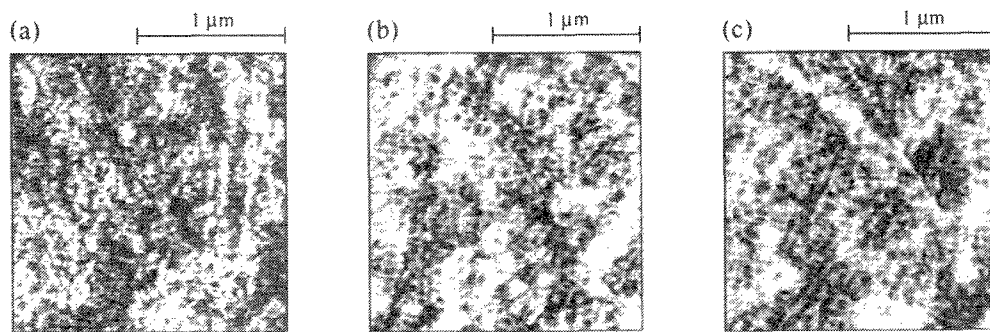


Fig. 4  $1.9\mu\text{m}\times 1.9\mu\text{m}$  CR-PFM images of the (001) plate PMN-PT single crystal observed after the sample was heated up to  $220^\circ\text{C}$  and then cooled down to  $50^\circ\text{C}$  at a rate of  $60^\circ\text{C}/\text{h}$ : (a) just after the sample was cooled down, (b) 9 hours passed, and (c) 18 hours passed.

the sample heating.

#### 4 CONCLUSIONS

We observed the domain structures of the (001) plate PMN-PT single crystal in a vacuum using CR-PFM with a view to clarifying the air convection effect. The same fingerprint-shaped domain images were observed below and above the Curie temperature, which was similar to the result obtained in the air. Therefore, it was revealed that surface temperature drop due to the air convection was not the reason why domain images were obtained above the Curie temperature. We also found spot-shaped domains tens of nanometers in diameter at temperatures above  $175^\circ\text{C}$ . Once these spot-shaped domains appeared, they were observed even below the Curie temperature and returned gradually to the larger fingerprint-shaped domains obtained before the sample heating. We believed that this long time relaxation phenomenon was connected with the relaxor characteristics.

#### Acknowledgements

We are pleased to express our gratitude to Dr. Yohachi Yamashita for providing excellent PMN-PT single crystals. This work was partly supported by Foundation for Promotion of Material Science and Technology of Japan (MST Foundation) and Kato Science Promotion Foundation.

#### References

- [1] G. A. Smolensky and A. I. Agranovskaya, *Soviet Phys.-Solid. State.* **1**, 1429 (1959).
- [2] G. A. Smolensky and A. I. Agranovskaya, *Soviet Phys.-Tech. Phys.* **3**, 1380 (1958).
- [3] J. Kuwata, K. Uchino, and S. Nomura, *Jpn. J. Appl. Phys.* **21**, 1298 (1982).
- [4] S. Park and T. Shrout, *IEEE Trans. Ultrason. Ferroelectr. Freq. Control* **44**, 1140 (1997).
- [5] S. Saitoh, T. Takeuchi, T. Kobayashi, K. Harada, S. Shimanuki, and Y. Yamashita, *IEEE Trans. Ultrason. Ferroelectr. Freq. Control* **46**, 414 (1999).
- [6] V. Westphal, W. Kleemann, and M. D. Glinchuk, *Phys. Rev. Lett.* **68**, 847 (1992).
- [7] N. Takesue, Y. Fujii, M. Ichihara, and H. Chen, *Phys. Rev. Lett.* **82**, 3709 (1999).
- [8] Y. Uesu, H. Takazawa, K. Fujishiro, and Y. Yamada, *J. Korean Phys. Soc.* **29**, S703 (1996).
- [9] P. Li, Y. Wang, and I. W. Chen, *Ferroelectrics* **158**, 229 (1994).
- [10] K. Nomura, T. Shingai, N. Yasuda, H. Ohwa, and H. Terauchi, *Ferroelectrics* **218**, 69 (1998).
- [11] Y. Yoshida, S. Mori, N. Yamamoto, Y. Uesu, and J. M. Kiat, *J. Korean Phys. Soc.* **32**, S993 (1998).
- [12] R. Luthi, H. Haefke, K. P. Meyer, L. Howald, and H. J. Guntherodt, *J. Appl. Phys.* **74**, 7461 (1993).
- [13] K. Takata, K. Kushida, K. Torii, and H. Miki, *Jpn. J. Appl. Phys.* **33**, 3193 (1994).
- [14] H. Okino, T. Ida, H. Ebihara, and T. Yamamoto, *Ferroelectrics* **268**, 119 (2002).
- [15] H. Okino, K. Yuzawa, K. Matsushige, and T. Yamamoto, *Trans. Mater. Res. Soc. Jpn.* **27**, 239 (2002).
- [16] K. Yamanaka, A. Noguchi, T. Tsuji, T. Koike, and T. Goto, *Surf. Interface Anal.* **27**, 600 (1999).
- [17] H. Okino, T. Ida, H. Ebihara, H. Yamada, K. Matsushige, and T. Yamamoto, *Jpn. J. Appl. Phys.* **40**, 5828 (2001).

(Received December 21, 2002; Accepted January 31, 2003)